



СООБЩЕНИЯ  
ОБЪЕДИНЕННОГО  
ИНСТИТУТА  
ЯДЕРНЫХ  
ИССЛЕДОВАНИЙ

Дубна

96-168

E9-96-168

ATLAS Internal Note  
TILECAL-NO-058

S.B.Vorozhtsov, I.V.Titkova, M.Nessi\*

CONTRIBUTION  
TO THE ATLAS B-FIELD 3D MODEL

---

\*CERN, Geneva, Switzerland

1996

# 1 Introduction

In a process of preparing the General Three Dimensional (3D) Computer Model (G3DCM) of the ATLAS magnetic field distribution [1], [2] one needs to perform a set of calculations, using simplified configurations, to get an idea of the effect of various system peculiarities on the G3DCM. It seems to be more efficient way to get such an estimation within above mentioned models than to use for this purpose the G3DCM itself with its limited resolution (limited number of nodes) and rather time consuming calculations. This way the effects under consideration can be chosen or rejected from the point of view of their importance for the G3DCM: current level of obtained and desired accuracy of the B-field estimation. In this Note mainly the TileCal part of the ATLAS B-field model is considered. Our results were obtained with the help of the TOSCA [3], OPERA-2D [4] and POISCR [5] calculations.

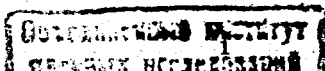
## 2 Glue Layers

New effect to be investigated for its possible introduction into the G3DCM (new anisotropic B(H) curves) -  $50 \mu$  glue layers between spacers and master plates. These layers could be considered as effective air gaps between above mentioned elements. At first glance due to these gaps there should be some modifications of the existing model, but the gaps value is too small in comparison with the characteristic iron plate thickness (5 mm, lamination packing factor 0.99) to change the previous TileCal B-field conception completely.

There is also no constant  $50 \mu$  glue gap in the structure. These gaps can vary from 0 to the maximum value  $50 \mu$ . The reason for that indicated in Ref. [6]. One can read there: "The glue gap has the role of keeping the stack solid and at the same time compensating for surface planarity defects". Under such conditions one should normally consider some RMS value, say,  $25 \mu$  gaps, but not the upper limit  $50 \mu$  gaps.

There are several TileCal features that could be affected by the introduction of the glue gaps into the structure:

- TileCal iron anisotropy.
- Active zone TileCal flux, passing through the  $Z=0$  plane.
- The laminated iron near girder efficiency for the solenoid flux conducting.



- PMT location field.
- Waving of the flux lines around the tiles in the active zone.
- $B_{tile}$  value.

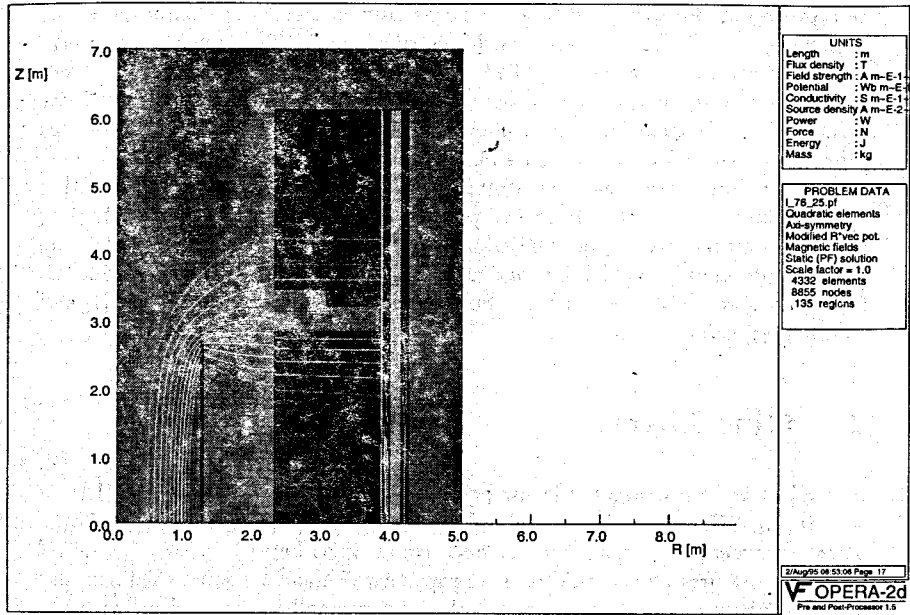


Figure 1: Distribution of the flux lines in the system.

General layout of the system is shown in Fig 1. There one can see the solenoid ( to the left) and TileCal structure elements (to the right): Barrel, Extended Barrel, Plug, Girder.

The OPERA-2D PF analysis program - a special version of non-linear magnetostatics program for laminated material defined with a packing factor (0.76 in this case) was used for this calculation and the other RZ-problems below. Glue gap values were 25  $\mu$  there.

TileCal iron was already anisotropic due to staggered tile structure. The question is how large are these glue gaps in comparison with the tile slot thickness

to increase substantially anisotropic property of the TileCal iron. To get an idea of that one should compare the packing factor 0.76 due to tiles and 0.99 due to glue gaps.

Active zone TileCal flux, passing through the  $Z=0$  plane, should decrease because of these glue gaps. POISCR calculation showed that the active zone flux, passing through the  $Z=0$  plane, got down on  $\approx 30 \div 40 \%$ . The largest value is a limiting case with the exaggerated anisotropy of the zone (laminated anisotropy with the packing factor 0.76).

One could imagine that the laminated iron near girder of radial dimension 71 mm might become useless for the solenoid flux conducting due to the glue gaps laminated anisotropy. But there is only 41 mm of pure laminated iron near the girder with the packing factor 0.99 for the 50  $\mu$  glue gaps. The other two layers of 10 mm and 20 mm radial dimensions have even higher packing factor due to straps and girder solid iron, incorporated azimuthally. Having in mind these facts and the larger fraction of flux directed to the girder due to the glue gaps effect we observed a higher than it has been calculated before induction value in solid iron of girder (Fig 2).

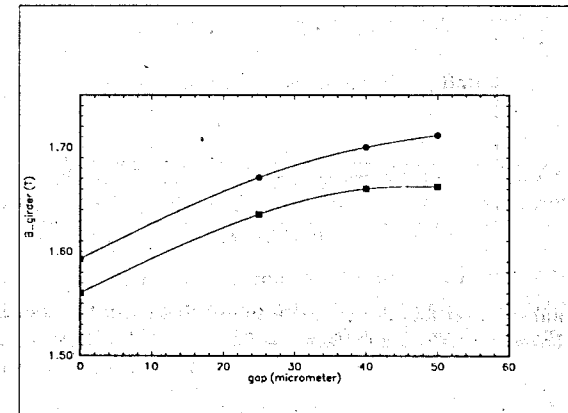


Figure 2: Girder field dependence on glue gap value. Circles - initial packing factor = 0.76, boxes - initial packing factor = 0.90.

In this Figure two initial (without glue gaps anisotropy) packing factors were

considered:

- 0.76 - tile structure exaggerated anisotropy,
- 0.90 - tile structure laminated anisotropy with the waving effects included.

As a consequence of the girder field level increase the pure laminated layer relative contribution to the total flux decreased in the worst case only on 22 % for 25  $\mu$  gaps and on 34 % for 50  $\mu$  gaps (Fig. 3, Fig. 4). For clarity in the Fig 4 the scale in the R-direction was enlarged substantially. The packing factor of the active zone was 0.76 and glue gaps 25  $\mu$  in this Figure.

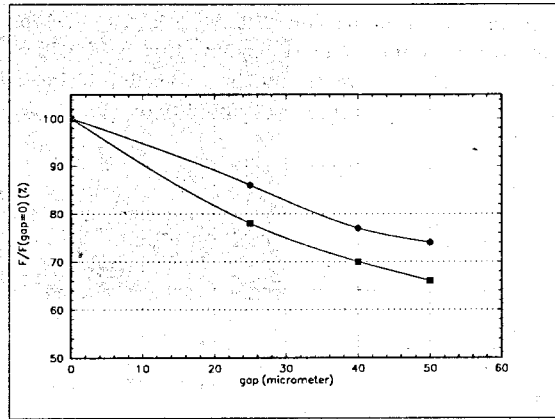


Figure 3: Laminated layer flux decrease due to the glue gaps. Circles - initial packing factor = 0.76, boxes - initial packing factor = 0.90.

Due to the increased flux to the girder the PMT location field would increase somewhat with the glue gaps inserted into the model. The estimation of the PMT field change, given in Ref. [1], still to be confirmed by independent calculations.

In the absence of a glue layers the magnetic flux will pass through a bottleneck of a few mm length, formed by the master plate and two neighboring spacers on each side of the master plate. The flux lines wave around the tiles [7] in the active zone. This effect permits rather large flux fraction to pass through the tile zone (Fig. 5).

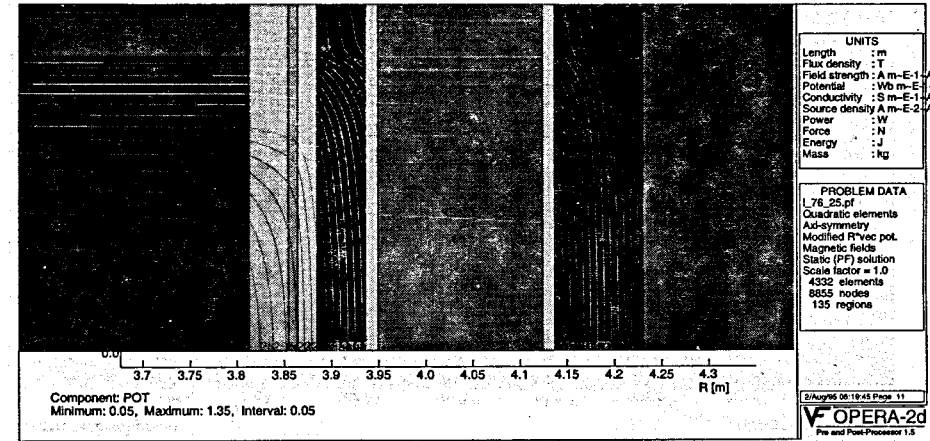


Figure 4: Flux map in the girder region of the Barrel.

For simplicity in this and following tile structure models the XOY coordinate system is used, with the X-axis directed as the R-axis in the real system and the Y-axis directed as the Z-axis in the real system.

To help better waving there were introduced 2 mm iron layers between tiles, along Z-axis in the system. Calculations with the help OPERA-2D show that with these 2 mm layers the highest field value zones situated near small regions at the very corners of the tiles (Fig. 5).

Without these layers the total area between adjacent tile rows is under the high field, thus increasing substantially the probability of flux lines penetration to the tiles (Fig. 6).

Calculation shows that even with 0.25 mm glue gaps there is still very perfect waving present in the flux line behavior (Fig. 7). For clarity in the figure the scale in the Y-direction is enlarged substantially.

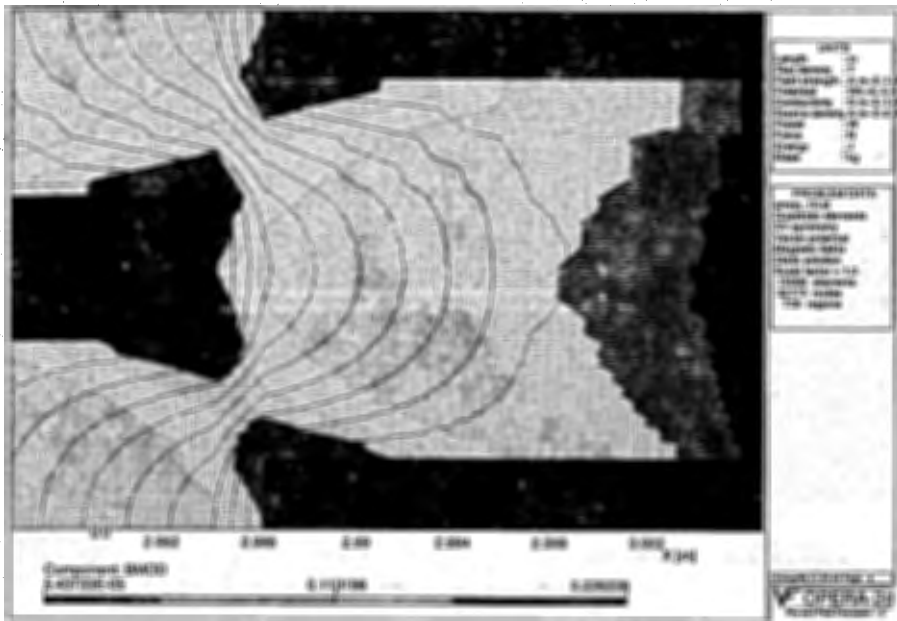


Figure 5: Flux map for no glue gaps and 2mm layers present in the system.

Due to above said one would not recommend to remove these layers from the TileCal active zone.

There are two factors which affect the  $B_{tile}$  value with the glue gaps in the structure. One of them - an iron shielding coefficient  $K_{shiel}$  (the ratio of the external field to the  $B_{tile}$  field) goes down with the increase of the glue gap value. This effect leads to the larger magnetic flux penetration to the tiles (compare Fig. 5 and Fig. 8).

The second one is an anisotropy increase, which diminishes the  $B_{normal}$  to the tile surface component value. POISCR calculation showed that the second factor is the major one in our case and that the  $B_{tile}$  values got down on 30 ÷ 80 % due to the fact that the larger part of the active zone flux goes tangentially to the tile surface and in the direction of the girder. These calculations still to be confirmed by the OPERA-2D cross-check.

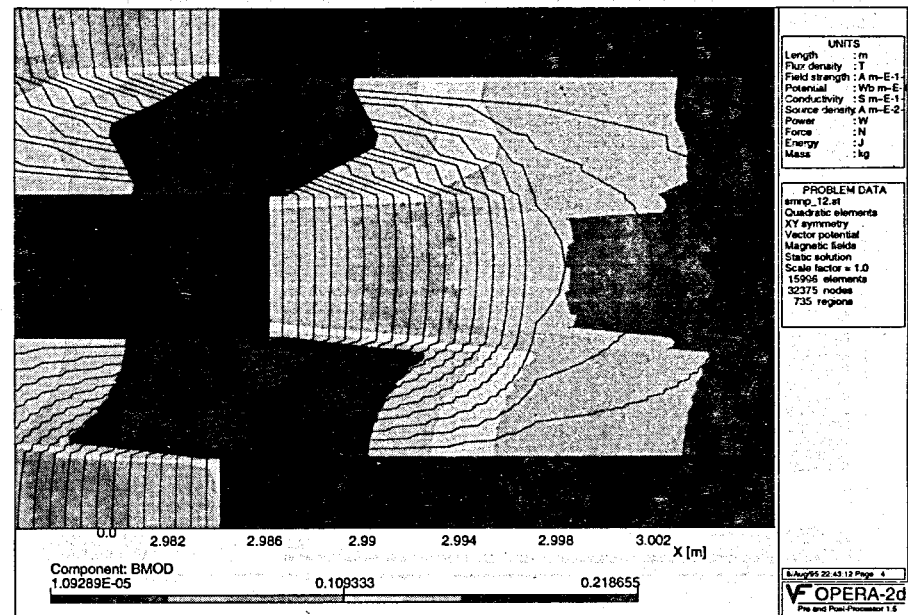


Figure 6: Flux map for no glue gaps and no 2mm layers in the system.

### 3 Magnetic Field Measurements

A TileCal segment was inserted into the MNP24 test magnet gap (20 cm) to measure the effect of tile shielding by iron [2]. It is interesting to try to get maximum information from these measurements. The main question to be asked there: what would be the  $B_{tile}$  values when the glue gaps are in the structure. Basing on this experiment the corresponding corrections could be introduced into the B(H) magnetic property performance of the TileCal, which is used for the G3DCM.

In Fig. 9 experimental data from in Ref. [2] for the external field value 105 Gs are given. From these data one can estimate that the characteristic shielding coefficient is  $\approx 2.4$  in this structure.

This very low shielding efficiency could be accounted for by the presence of 50  $\mu$  glue gaps in the system. But the OPERA-2D calculations using the model,

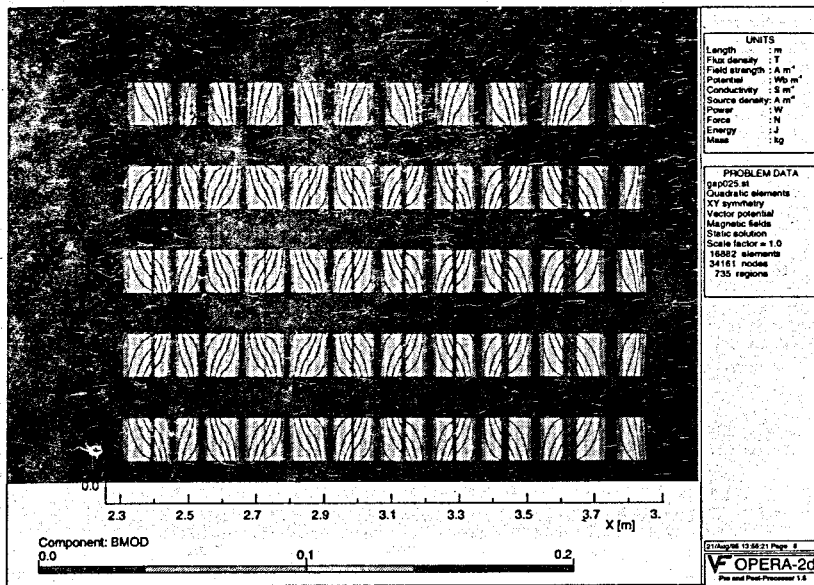


Figure 7: Flux lines waving around tiles with the 0.25 mm glue gaps in the system.

shown in Fig. 7, gives the shielding efficiency value 2.4 for gaps value  $\approx 0.6$  mm.

As far as  $50 \mu$  gaps concerned an analytical estimation for low field limit (infinite permeability of iron) gives the shielding efficiency  $\approx 20$ . Of course, the smaller glue gap value, the more  $K_{shield}$  goes down as compared with the low field limit due to the increased part of the flux going to the spacers and higher saturation of the master plate part just opposite the spacer corner (Fig. 8). Direct OPERA-2D calculation for the  $50 \mu$  gap is rather difficult due to finite size of the mesh cells. Indirect estimation for this gap value could be obtained by interpolation between no gap and somewhat bigger gap, still allowed for meshing, cases.

Actually, the structure under consideration has been undergone the mechanical reliability test and has been destroyed substantially. The planarity of the plates is very poor and the gaps between plates could be rather big as compared with  $50 \mu$  glue gaps.

A new set of measurements for the normal but not broken submodule in the

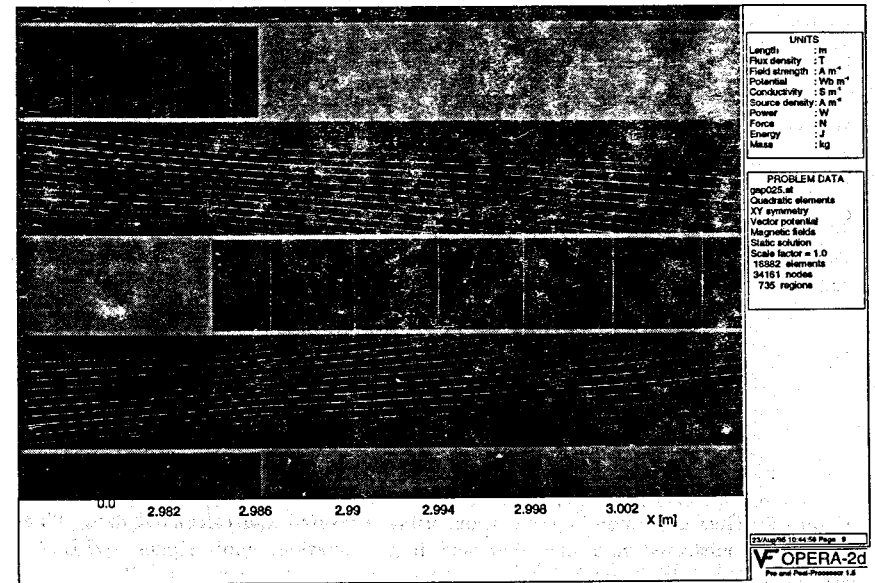


Figure 8: Flux map for 0.25 mm glue gaps.

magnet gap larger than 30 cm should be performed. Comparing the shielding efficiency measured and calculated one could define an actual effective glue gap value in the structure.

#### 4 End Plates, Front Plates

The total cross section of all end plates and front plates is about 20 % of the solenoid cross section, where from the total flux comes. So their usage for the flux conducting is of some interest.

The end plates are very essential to protect the tiles from the penetrating B-field in the crack region. When they are removed the  $B_{tile}$  increases fairly up 100 Gs. Their role is not only to conduct the flux to the girder but mainly to change the direction of the B-field from the normal to the tile surface to the tangential

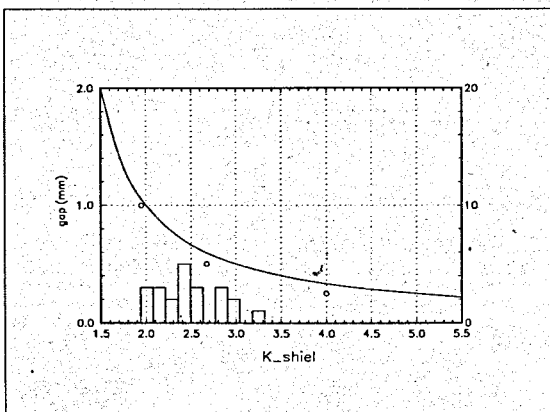


Figure 9: Glue gap value determination, using measured and calculated data. The histogram - measured data, line - low field limit estimation, empty circles - OPERA-2D calculation.

one. This decreases very much the  $B_{tile}$  in the adjacent regions. The front plates have the minor effect on the  $B_{tile}$  than the end plates. A detailed analysis of the effect of these structure elements on the TileCal magnetic field is given in Ref. [8].

The recent POISCR calculations, devoted to the end plates, attached to the Extended Barrel crack region side, show that the thickness of these end plates could be decreased from 2 cm to 1 cm with the corresponding corner  $B_{tile}$  value increase from 40 Gs to still tolerable 90 Gs.

The alternative solution could be a calibration of these few tiles with the B-field greater than 100 Gs.

## 5 TileCal Structure Details, Waiting to be Estimated

Measured  $B(H)$  for the anisotropic cold rolled steel of module-0 should also be reflected in the model. A precise measurement of the  $BH$ -curves of the iron of

girder and TileCal active is necessary. In connection with this one should mention the  $B(H)$  measurements of 4 mm and 5 mm cold rolled plates for the module-0, just recently performed in Dubna, the JINR [9].

There are also 0.35 mm air gaps between 30 cm submodules along Z-axis and 1 mm ÷ 5 mm air gaps between the master plates and between spacers of the adjacent modules respectively.

One should also take into account the holes for PMTs in the drawer and complicated girder structure at the interface between the Barrel and Extended Barrel. All these system peculiarities need tests on the simplified models of the TileCal.

## 6 Towards a General Atlas Field Map

The main ideas of this section subject have been discussed in Refs. [10] and [11]. Here we just shall give some additional considerations for performing the task of the field map preparing.

The first try to use the "toscab" information of the G3DCM has shown that for an adequate B-map presentation within the only one grid of the observation points would require an enormous amount of the computer time and disk space. So one should try to use the peculiarities of the detector field behavior to prepare the map in a most efficient way. The simplest and most natural way to do this is to subdivide the whole detector into three parts of different B-field structure with the separate observation points grid. Those parts could be: solenoid, TileCal, toroids regions.

The reasons for such a subdivision are the following:

It is not quite clear why one should spend computer time and finally get rather poor 3D, limited number of nodes meshing (less than  $\approx 100,000$  within the TOSCA) in the solenoid and in the some area of TileCal. This region could be very accurately described (at least at the given level of the B-field approximation) within a pure 2D model with the help of OPERA-2D. With this software one has a limit of the node number of order 100,000. Even in the case with a rather moderate 3D model number of nodes in azimuthal direction, for example - 10, the above mentioned 2D model number of nodes would be equivalent to the 100,000 nodes of the identical 3D model.

The most difficult part is the TileCal region. One should superimpose the grid over  $45^\circ$  azimuthal range to get the necessary approximation of the field map there [1]. In the TileCal part the accuracy of the field knowledge is still

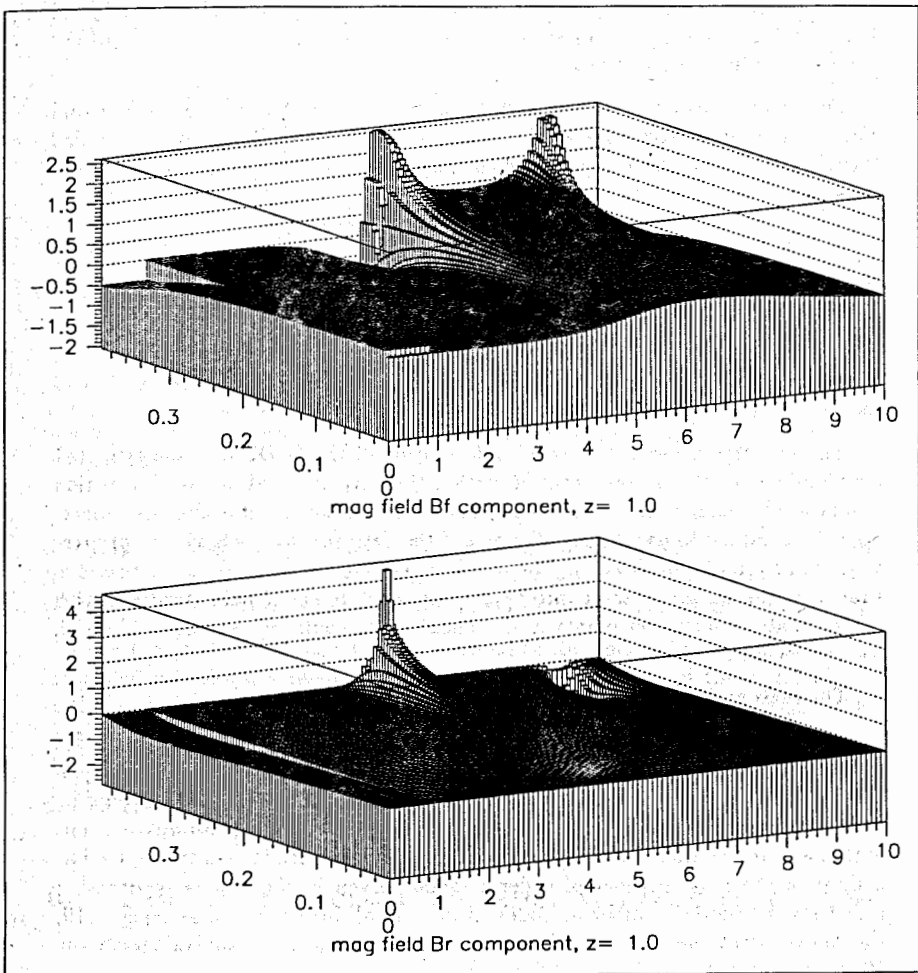


Figure 10: B values (Tesla) - map for  $Z=1m$ . Radius varies from 0 to 10 m. Azimuthal coordinate - from 0 to  $\pi/16$ .

rather poor ( $\approx 20\%$ ) and waiting to be improved substantially.

Less difficult than TileCal part is the toroids region. One should cover this region with the grid over the  $22.5^\circ$  azimuthal range only. There already exists some version of the B-field map for this part [12] with the rest of the volume has just zero field. In Fig. 10 one can see an example of the current B-field distribution for  $Z=1m$  coordinate plane.

Of course there should be overlapping between above mentioned adjacent parts as to insure the continuous behavior of the the corresponding fitting procedures throughout the whole detector with the help of suitable weighted sum of the considered field models.

The main goal of this work and following activity on the ATLAS magnetic field simulation is to fill the empty "desert" in the TileCal and solenoid area, like those shown in Fig. 10, with a decent realistic field map.

## 7 Conclusion

- Glue layers effect investigation shows that there should be some modifications of the existing model, but the total change of the previous TileCal B-field conception is not needed.
- Magnetic measurements of the tile shield efficiency gave an information about the actual glue gap values in the TileCal segment under test. It was found that the glue gaps there were much larger than the assumed  $50 \mu$  and a new set of measurements should be done.
- Due to the end plates and front plates importance for the field distribution in the corners of the crack region they should be included into the suitable version of the field model to match an obtained level of the accuracy of the TileCal field estimation.
- The construction of the General Atlas Field Map and magnetic field effects evaluation became the highest priority issue presently. A lot a work should be done to reach the necessary accuracy of the detector magnetic field distribution.

Authors acknowledge many stimulating discussions with Dr.F.Bergsma on the subject of this work. Authors also would like to thank Dr.P.Nevski for providing access to the existing ATLAS B-field map.



## References

- [1] F.Bergsma. Calculation of the ATLAS Magnetic Field TILECAL-NO-054, 16 August 1995.
- [2] F.Bergsma. Magnetic Model for ATLAS, Improvements on Tile-calorimeter Model. Transparencies shown at the Toroid Meeting (Magnetic Field) held at CERN, 12.07.95.
- [3] TOSCA Reference manual. Version 6.5. VF-11-94-14.
- [4] OPERA-2d Reference manual. Version 1.5. VF-11-94-24.
- [5] CERN Program Library Write-up T602.
- [6] Construction and Performance of an Iron-Scintillator Hadron Calorimeter with Longitudinal Configuration. RD-34 collaboration. CERN/LHCC/95-44. LRDB status report /RD34. 16 August 1995.
- [7] M.Nessi et el. TileCal Magnetic Field Simulation. ATLAS TILE-TR-013, June,1994.
- [8] S.V.Vorozhtsov et el. Influence of the TileCal Parameter Modifications on the B-field. TILE-No-50, 03-05-1995.
- [9] V.V.Kalinichenko, S.B.Fedorenko. Magnetic Property Measurements of Steel for TileCal. TILECAL-NO-05\*, 24 August 1995.
- [10] M.Nessi. Towards a General Atlas Field Map. Transparencies shown at the ATLAS physics workshop in Trest, June 12 ÷ 16, 1995.
- [11] M.Nessi. Requirements on the Field Knowledge. Transparencies shown at the Toroid Meeting (Magnetic Field) held at CERN, 12.07.95.
- [12] G.Poulard. On DICE Update. Version 2.04/01, 1/06/95/. "New Magnetic Field Map". July 6, 1995. CERN.ATLAS.COMPUTING news.

Received by Publishing Department  
on May 16, 1996.